

Study on the microstructure influence in ultrasonic test in duplex forged components

S. Barella, C. Di Cecca, A. Gruttadauria, C. Mapelli, D. Mombelli,
C. Fanezi Da Rocha, T. Strohaecker

Ultrasonic tests are fundamental to grant the integrity of the metal products, especially after forging operations. Due to the high attenuation of duplex stainless steel (DSS), the efficiency of ultrasonic test (UT) performed on DSS components could decrease and make the inspection difficult.

The interaction between the ultrasonic acoustic radiation and the microstructure of 2205 duplex stainless steel was studied. The specimens were treated at 780 °C for different soaking times to promote the precipitation of intermetallic phases. The UT response of each specimen was measured and associated to the corresponding microstructural features.

Electron Back Scatter Diffraction (EBSD) was performed to analyze the grains orientation and to relate the revealed crystallographic texture with the acoustic signal attenuation.

Tensile test were performed to determine the variation of the main mechanical parameters (yield strength, ultimate tensile strength, elongation and Young modulus) induced by the presence of the secondary phases.

The variation of ultrasound velocity can be associated to the modification of the volume fraction of the precipitated intermetallic phases (σ and χ phases) and to the morphology of the structural constituents observed within the material.

Keywords: Duplex stainless steel - Forging - Non-destructive Test - Ultrasonic test - Attenuation - Intermetallic phases

INTRODUCTION

The duplex stainless steel (DSS) family was introduced approximately 70 years ago, and its applications have continuously increased. DSSs have been applied in the chemical, oil and gas industries and in cellulose and paper manufacturing because this particular stainless steel has exceptional resistance to corrosion and good mechanical properties [1-4] due to the microstructure formed by ferrite, which provides high strength, and austenite, which provides toughness even at low temperatures.

If exposed to high temperatures, this alloy can be affected by undesirable problems [5], i.e., embrittlement at 475 °C and the precipitation of secondary phases, such as the χ phase, σ phase or carbides [6,7]. These intermetallic phases could be the activation factor for severe material damages affecting the mechanical properties [8,9,10] and the corrosion resistance [11]. Thus, this material should not be considered for its intermetallic phases and an inspection should be realized with attention.

Ultrasound is a tool widely used in industry for inspection because it is an efficient non-destructive technique [12] that allows the identification of the size and the position of a defect within the bulk of a component. Moreover, it is widely used as a support tool to verify the integrity of equipment such as boilers, pressure vessels, welds and valves. Using this technique, it is possible to obtain information about the microstructure, elastic constants and other mechanical properties of the materials.

Ultrasound intensity is dependent on the material bulk, which may attenuate its radiation energy and thereby affect the ultrasound propagation velocity. The phenomena ruling the attenuation of ultrasound radiation are due to diffraction, scattering, absorption mechanisms, thermoelastic relaxation, electron phonon interaction, phonon interaction, magnon-phonon interaction, lattice imperfections and grain boundary losses [13,14]. The most common

Silvia Barella, Cosmo Di Cecca, Andrea Gruttadauria, Carlo Mapelli, Davide Mombelli

*Dipartimento di Meccanica, Politecnico di Milano,
Via La Masa 34, 20156 Milano, Italy*

Claudia Fanezi Da Rocha, Telmo Strohaecker

*Universidade Federal do Rio Grande do Sul,
Avenida Paulo Gama, 110 - Farroupilha, Porto Alegre, Brazil*

*Paper presented at the 2nd International Conference Ingot Casting Rolling and Forging - ICRF 2014,
Milan 7-9 May 2014*

methods of ultrasonic examination utilize shear waves or, in this case, longitudinal waves.

This work aims to study the response of forged duplex stainless steel affected by intermetallic phases precipitation when inspected by ultrasound. Actually, during the subsequent forging steps, the work piece is plastically deformed up to the temperature reaches a thermal level no more suitable to continue the hot-forge process and then is re-heated approximately at 950 °C. During this time, the temperature passes through the precipitation range of the intermetallic phases. Thus, a residual fraction of intermetallic compounds could remain in the final components, afflicting both the mechanical properties and the ultrasound response. Moreover, the experiments aimed to evaluate the possibility to use UTs as a method to quantify the residual intermetallic fraction in forged DSS components.

To perform this analysis, the studied alloy was thermally heated for different durations to induce the precipitation of the intermetallic phases. Then, the treated specimens were analyzed to obtain a complete characterization, as shown in the results.

EXPERIMENTAL PROCEDURE

The investigation was performed on UNS S31803 (Table 1) duplex stainless steel bar obtained by forging and then solubilized. Different samples of 45×45×15 mm in size were obtained.

C	Cr	Mn	Mo	N	Ni	P	S	Si	Al
0.0240	22.14	1.79	3.38	0.17	5.11	0.02	0.0005	0.55	0.018

Table 1 – Chemical composition of the investigated duplex stainless steel (wt.%).

Tabella 1 – Composizione chimica dell'acciaio inossidabile duplex studiato (% in peso).

The different samples were heat treated at 780 °C for different treatment time and water cooled to induce the precipitation of different volume fractions of the intermetallic phases (Table 2).

Metallographic analyses were performed to measure the volume fraction of the different precipitated phases. These analyses were based on the data collected by optical microscopy on different metallographic samples. The specimens used for optical investigations were cut, polished and etched by applying a modified Beraha etching solution (20 ml HCl, 80 ml distilled water, 1 g K₂S₂O₅ and 2 g NH₄HF₂) for 5 s. Image analysis software was used to quantify the different phases. A ferritoscope Fisher MP 30 was used to measure the ferrite content.

SEM study was carried out to characterize the morphology and the nature of the precipitated phases, exploiting the EDS probe coupled with the microscope.

The grain misorientations were measured by EBSD analysis [15] and their influence on wave attenuation was estimated. The surfaces of the examined samples were pre-

Sample	Time of treatment (minutes)	Water cooling
A	As-received	
B	10	
C	30	
D	60	
E	120	
F	180	
G	240	
H	300	
I	390	
J	480	
K	600	

Table 2 – Sample identification and investigated experimental conditions

Tabella 2 – Identificazione campioni e condizioni sperimentali investigate.

pared using a polishing solution of 0.05 μm colloidal silica suspension distributed on a cloth. The working parameters of the SEM–EBSD system were set at an accelerating voltage of 20 keV and observed at a 200x magnification corresponding to a pixel size of 25 μm². The integration time for the interpretation of the diffraction pattern was varied between 5 ms to 7.5 ms.

From EBSD analysis, the CSL (coincidence-site lattice) numbers were also measured. These are a geometrical construction based on the geometry of the lattice that two grains have when they are misoriented by an angle θ around an axis *o*.

The density of coincidence sites, or better, its reciprocal value is an important parameter characterizing the CSL. Choosing an elementary cell, CSL number (Σ) is determined by:

$$\Sigma = \frac{\text{number of coincidence sites} \in \text{an elementary cell}}{\text{total number of all lattice sites} \in \text{an elementary cell}} \quad (1)$$

The main Σ values investigated in this work were Σ3 and Σ13. The first accounts to twinning occurring in the FCC phase present in the duplex stainless steel whereas the latter is associated to recrystallization in ferritic phase and for these reasons both are important since any changing in this parameters interfere on the response of ultrasound, modifying the ultrasonic velocity.

Tensile test has been performed to investigate the influence of intermetallic phases on the mechanical properties of material using a Instron 5585H – 250 kN tensile testing machine. The yield strength, ultimate tensile strength, elongation and Young modulus were measured for all the experimental conditions. The presence of intermetallic phases generally affect these properties, reducing the performance of the in service components.

In particular, the Young modulus behavior was investigated,

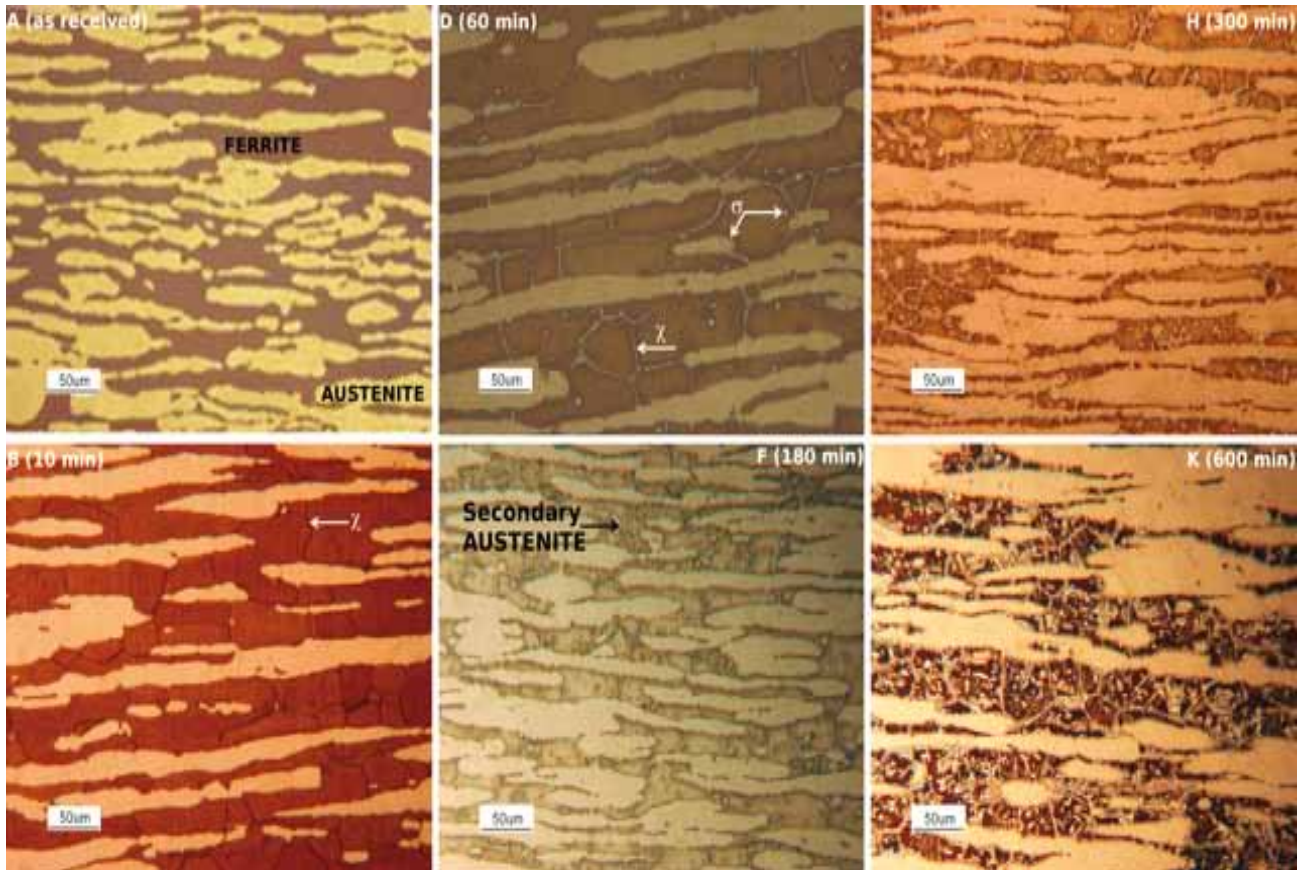


Fig. 1 – Metallographies at different treatment times.

Fig. 1 – Metallografie a differenti tempi di trattamento.

because its changing causes alteration on the ultrasound velocity of material, since this two parameters are dependent each other as reported in equation (2) [ASMT E494-10],

$$E = \frac{\rho \cdot v_t^2 \cdot (3v_l^2 - 4v_t^2)}{v_l^2 - v_t^2} \quad (2)$$

where E is the Young modulus, v_t is the transverse sound velocity, v_l is the longitudinal sound velocity and ρ is the steel density.

Longitudinal ultrasonic velocity measurements were performed on the different samples to correlate the attenuation with the microstructure of each sample. The measurement was performed by a Gilardoni RDG 800 instrument with 4 MHz contact straight beam probe.

Ultragel was used as a couplant for the probe to eliminate the air gap between the transducer and test specimen and to provide an efficient transmission of the waves from the transducer to the material.

RESULTS

The metallographic analysis results are reported in Figure 1. The applied reagent reveals the presence of ferrite, austenite, secondary austenite and intermetallic phases. The ferrite phase is dark and the austenite phase is light. The secondary austenite phase is detectable because of

its characteristic elongated morphology. The other phases are white when observed by optical microscope. The χ phase is concentrated at the grain boundaries [16] during short treatment times. The σ phase is also located at the grain boundaries; however, after a long heat treatment, this phase could precipitate within the ferrite and the austenite grains.

The as-received material contained approximately the 40% volume fraction of ferrite and 60% volume fraction of austenite (Figure 1 - sample A). After the different treatment times at 780 °C, the intermetallic phases precipitated, changing the microstructure and the volume fraction of the phases.

As shown in Figure 1 - sample B, after 10 minutes of treatment, the χ phase decorates the grain boundary of the ferrite phase with an elongated morphology. The precipitation of χ -phase generally occurs before the σ -phase precipitation. Only after 30 minutes of treatment, the σ phase starts to precipitate at the grain boundary, also consuming the ferrite [17-18]. The χ -phase precipitation continues at the ferrite/ferrite interface, then, both phases coexist in the microstructure. Further increasing the treatment time, the σ phase starts to precipitates also inside the ferrite grains [17] (Figure 1 - sample D). It is possible that the χ and σ phases occur together in the material until 180 minutes of treatment. After this condition, every χ phase is consumed and transformed into the σ phase [19]. The σ -phase for-

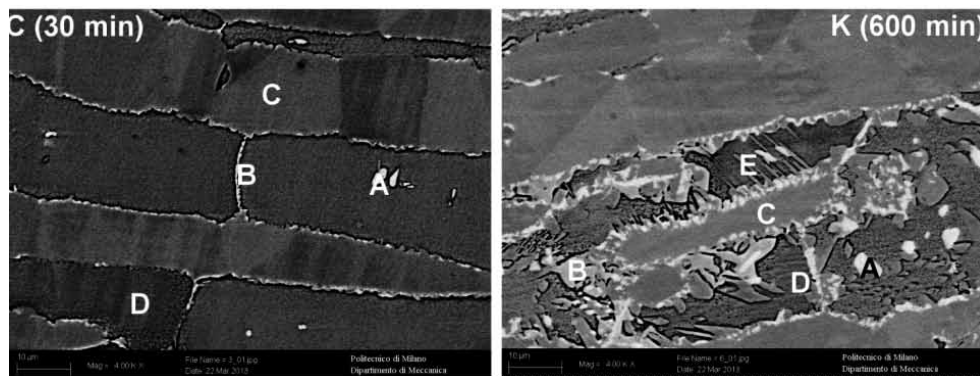


Fig. 2 – SEM-BSE microographies of sample C treated for 30 minutes (right) and sample K treated for 600 minutes (left).

Fig.2 – Micrografie SEM-BSE del campione C trattato 30 minuti (destra) e del campione K trattato 600 minuti (sinistra).

mation in ferritic/austenitic duplex stainless steels can be represented by an eutectoid type reaction of ferrite giving σ -phase and austenite as follows: $\delta \rightarrow \sigma + \gamma'$, where γ' is known as secondary austenite. This reaction may totally consume the ferrite phase of the steel. σ -phase nucleated mainly at ferrite/austenite interface and grew inwards into the ferrite phase. Sigma phase precipitates also at ferrite/ferrite grain boundaries. Secondary austenite formation becomes evident only after 3 hours of treatment (Figure 1 - sample F). Further increasing in treatment time lead the progressive consumption of the ferritic phase in favor of secondary austenite (that grows and coalesces) and σ phases precipitation (Figure 1 - sample H and K).

EDS chemical analyses were performed on all the treated samples to verify the chemical composition of the different phases recognized on the basis of their morphology (Figure 2, Table 3), especially the intermetallic phases. The presence of the χ phase (in particular, for samples B to F), σ phase and secondary austenite can be easily identified on the basis of BSE (back scattered electrons) contrast in SEM because χ phase is richer in the heavy element Mo than σ phase and hence is the brightest one. As indicated by the SEM-EDS analysis, the χ phase presents more molybdenum and less chromium than the sigma phase [6,10,20]. The volume fraction of each phase is shown in Figure 3.

The volume fraction of the phases was measured by image analysis. The value of the ferrite volume fraction was obtained by subtracting the volume fraction of the other observed phases. The obtained value corresponds with the value obtained through the ferritoscope measurement; this is a significant result indicating the reliability of the performed measurements.

The volume fraction of the austenite manifests the typical oscillating behavior imposed by isothermal heat treatment. The trend is due to the inertia of diffusion and consequently to the inertia of microstructure changing. During annealing, diffusion takes place acting to homogenize the chemical composition and allowing the balance of the phase amount (according to the thermal level) by the nucleation and growth of new grains. In the first annealing period, diffusion phenomenon is favourite because of the non-homogeneous chemical composition due to the fast cooling rate of the previous annealing. Moreover, the austenite volume fraction takes into account also the formation of secondary austenite, induced by the eutectoid transformation from δ phase to σ phase. On the contrary,

Sample C (30 min)	Cr (wt.%)	Mn (wt.%)	Ni (wt.%)	Mo (wt.%)
A (σ)	29.60	1.89	4.80	8.10
B (χ)	26.74	1.95	3.74	13.04
C (austenite)	21.68	2.16	6.26	2.01
D (ferrite)	24.52	1.97	6.20	4.10
Sample K (600 min)	Cr (wt.%)	Mn (wt.%)	Ni (wt.%)	Mo (wt.%)
A (σ)	27.50	1.96	3.95	9.79
B (σ)	28.01	1.84	4.20	9.50
C (austenite)	21.56	2.10	6.25	2.99
D (ferrite)	26.70	1.58	7.20	2.43
E (secondary austenite)	22.40	2.57	5.20	1.75

Table 3 – SEM-EDS local chemical composition of the phases identified in Fig. 2.

Tabella 3 – Composizione chimica locale mediante SEM-EDS delle fasi identificate in Fig. 2.

the volume fraction of ferrite progressively decreases as the intermetallic volume fraction increase [18]. As reported in literature [19,21,22], sigma phase formation occurs in ferrite, consuming practically all the ferrite in the steel. The high susceptibility of the duplex stainless steels to the sigma phase formation is frequently attributed to the ferrite composition, richer in the sigma forming elements (Cr, Mo and Si) and poorer in the elements that are less soluble in sigma (C, N and Ni) than in austenite. Moreover, the occurrence of the eutectoid reaction seems to demand a minimum amount of austenite (gammagenic) forming elements (mainly Ni, N and C) in the steel composition. The new austenite formed in the eutectoid reaction is poorer in Cr, Mo and N than the original austenite (Table 3) and this causes considerable drop in the corrosion resistance of the steel [23].

Another important parameter that can be evaluated from microstructural analysis is the ferrite lamellae thickness. Four lines were drawn on each metallographic analysis, and the thickness of the lamellae and the number of interceptions among the lines and the lamellae were counted.

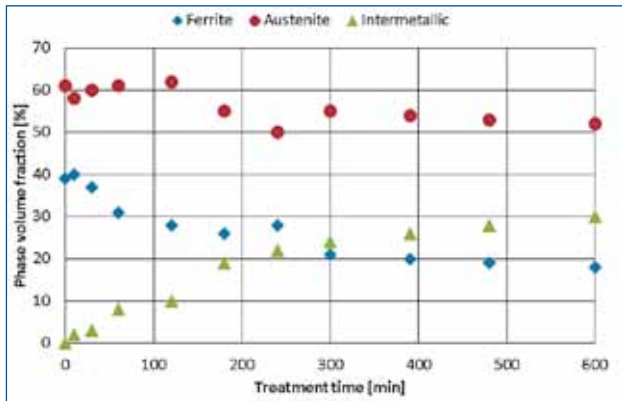


Fig. 3 - Phase volume fraction at different treatment times.

Fig. 3 - Frazione volumetrica delle diverse fasi in funzione del tempo di trattamento.

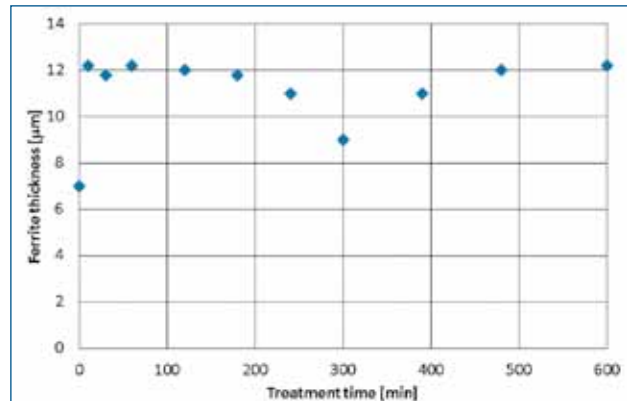


Fig. 4 - Ferrite lamellae thickness as a function of the treatment time.

Fig. 4 - Spessore delle lamelle di ferrite in funzione del tempo di trattamento.

The lamellae thickness values are reported in Figure 4. With changing treatment duration, the thickness featuring the ferrite lamellae changes: beginning with the shortest treatment duration, the thickness of the ferrite lamellae decreases progressively up to 300 minutes of treatment. This is due to the decrease of ferrite content and the corresponding nucleation and growth of the intermetallic phases. For the longest treatment duration, the ferrite lamellae become thicker because the volume fraction of the intermetallic phase increases not only on the ferrite grain boundaries but also within the grain cores. The nucleation and the growth of the intermetallic phase within the ferrite grains decreases the width of each ferrite lamella because each lamella is separated by the layer of the growing intermetallic phases.

EBSD analysis quantified the misorientation of the grain boundaries by measuring the rotation angle describing the misalignment of the lattices between the adjacent grains. In Figure 5, the misorientation induced by the different applied heat treatments are indicated; the misorientation of untreated sample, 60-minutes treated sample, 300-minutes treated sample and 600-minutes treated sample are reported. All the specimens treated for more than 60 minutes, are interested by the presence of intermetallic phases. Increasing the treatment time, the fraction of grain boundaries featured by low misorientation angle increases, too. This aspect, associated to the high fraction of grains featured by low misorientation angles (Figure 6), means that the material has been strongly oriented. Moreover, the precipitation and growth of intermetallic phases at the boundary and within the grains, and the subsequent formation of secondary austenite contribute to increase the number of grains characterized by low misorientation, since these new phases interrupt the continuity of ferritic phases.

The CSL number has been measured and the ratio between $\Sigma 13$ and $\Sigma 3$ grain boundaries has been estimated (Figure 7). The $\Sigma 13/\Sigma 3$ ratio points out a decreasing behavior as a function of the heat treatment time. This means that the

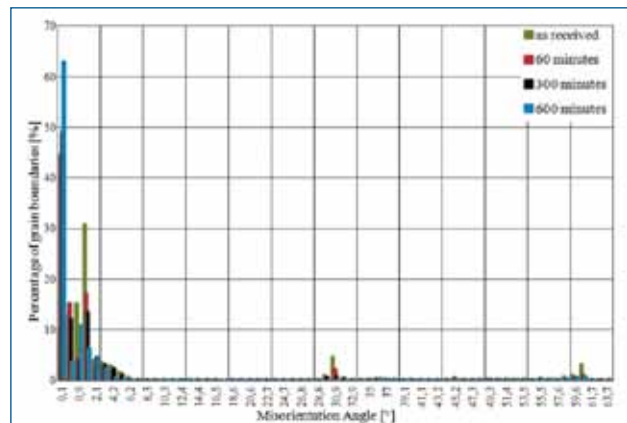


Fig. 5 - Misorientation angles determined by EBSD.

Fig. 5 - Angoli di misorientazione determinati mediante analisi EBSD.

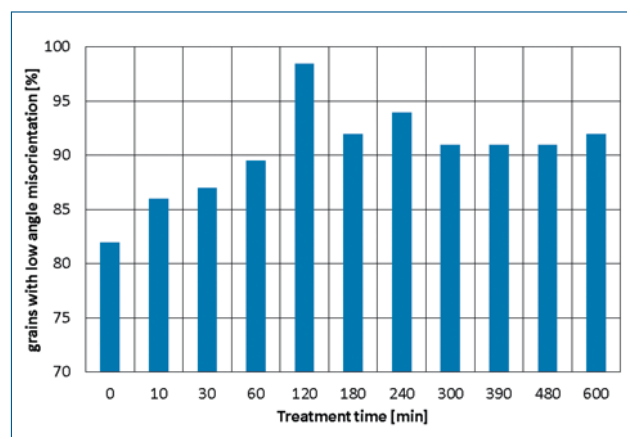


Fig. 6 - Number of grains with low angle misorientation in relation to the treatment time.

Fig. 6 - Numero di grani con bassa misorientazione in funzione del tempo di trattamento.

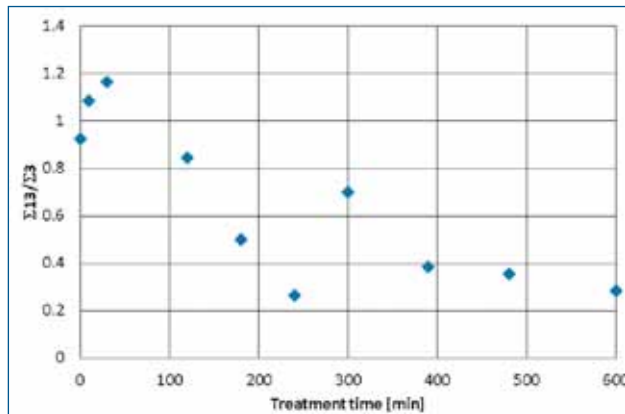


Fig. 7 - Ratio between Σ_{13} and Σ_3 as a function of the treatment time.

Fig. 7 - Rapporto fra Σ_{13} e Σ_3 in funzione del tempo di trattamento.

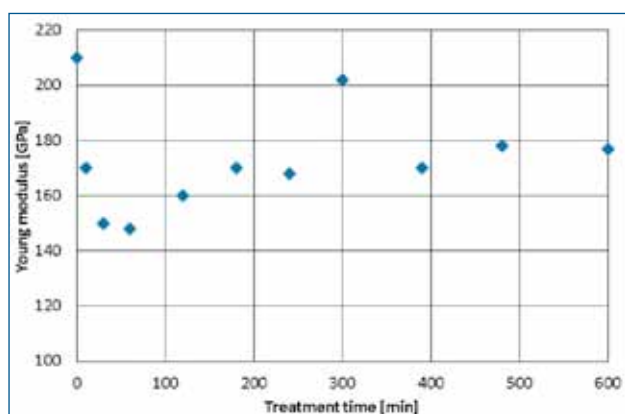


Fig. 9 - Young modulus of the investigated samples as a function of the treatment time.

Fig. 9 - Modulo di Young dei campioni investigati in funzione del tempo di trattamento.

recrystallization that takes place in the ferritic phase at the shorter treatment time is then balanced by twinning phenomena. However, this ratio unexpectedly shoots up after 300 minutes of treatment. Probably, for the short heat treatments, the plastic deformation energy stored in the material is enough to promote the refinement of the microstructure [23]. The new ferritic grain boundaries promoted by the recrystallization became the preferential sites where χ phase starts to precipitate (Figure 1 - sample B and D). When the secondary austenite formation becomes important (after 180 minutes), the orientation of the γ'' islands could be interpreted by EBSD like a twinned austenitic grains, hence the Σ_3 value increases.

The relationship between yield strength, tensile strength, elongation at the fracture point and treatment time is shown in the Figure 8. The yield strength (YS) and the ultimate tensile strength (UTS) are nearly constants and they seem to be not affected by the presence of intermetallic phases. However, increasing the volume fraction of intermetallic phases, a weak strain hardening of the material is pointed out, except at 300 minutes, where the investigated

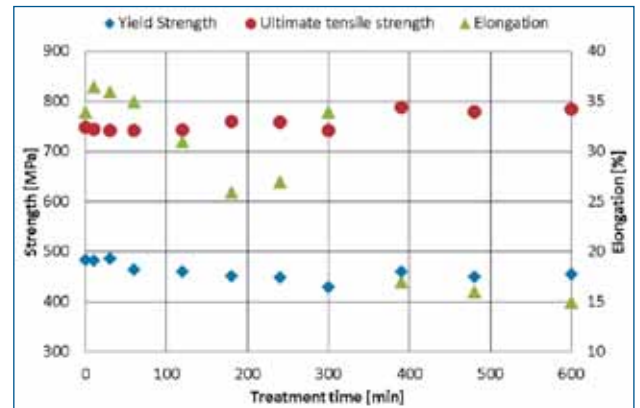


Fig. 8 - Relationship between yield strength, ultimate tensile strength and elongation at the different treatment times

Fig. 8 - Relazione fra carico di snervamento, carico di rottura e allungamento % per i differenti tempi di trattamento.

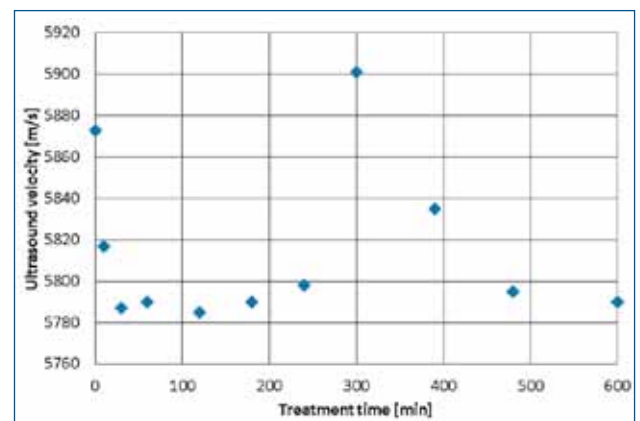


Fig. 10 - Longitudinal ultrasound velocity as a function of the treatment time.

Fig. 10 - Velocità ultrasonica longitudinale in funzione del tempo di trattamento.

alloy seems to soften. On the contrary, the elongation and Young modulus (Figure 9) have significantly changed. The intermetallic phases precipitation could induce important variation in elongation and Young modulus, especially when their volume fraction is above the 15-20% [25]. The elongation monotonically decreases, increasing the intermetallics volume fraction, and this result is consistent with the literature [10,25]. However, both the elongation and the elastic modulus shot up in correspondence of 24% of intermetallic phases (300 minutes of treatment). This Young modulus variation coincides with the changes observed on the ultrasound velocity. The higher elastic modulus is associated with the higher ultrasound velocity (Figure 10).

For the as-received sample, the ultrasonic velocity is 5873 m/s. The ultrasound velocity decreased for the samples thermally treated up to 240 minutes that is associated with a volume fraction of the precipitated intermetallic phases of 22%. For the samples thermally treated for 300 min-

utes, the volume fraction of intermetallic phases is about 24% and the ultrasonic velocity increased to 5901 m/s and then subsequently decreased, when the volume fraction of intermetallic phases is about 26% until 30%. Such a precipitated volume fraction of the intermetallic phases coincides with a strong decrease of $\Sigma 13/\Sigma 3$. Moreover, the peak in ultrasound velocity revealed at 300 minutes corresponds with the unexpected variation of the main parameters investigated in this work: Young modulus, elongation, and ferrite lamellae thickness. The microstructural features reached after 300 minutes seem to grant the lowest attenuation in ultrasound test.

DISCUSSION

The results obtained show the different behavior of the different treated samples and could be related with their microstructural changes. As the treatment time increased, the amount of intermetallic phases increased, as expected. At the same time, the ferrite morphology changed, also decreasing the ferrite volume fraction. The thickness of the ferrite lamellae remained constant for the short treatment time (from 10 minutes to 60 minutes). For the long ageing (from 60 minutes to 300 minutes), the ferrite lamellae thickness slightly decreases. This variation in ferrite morphology seems strongly related with the variation observed in ultrasound velocity measurement. Indeed, after a sufficient time, the formation and growth of secondary phases reduce the ferrite amount resulting on decrease in the ultrasound velocity. On the other hand, for the short heat treatment, the ferrite recrystallization took place, reducing the ferritic grain size. Even if the finer microstructure should improve the material transparency [26], the progressive intermetallics precipitation contribute to increase the UTs attenuation because the ultrasonic waves undergone to higher dispersion for scattering, due to the high number of phase interfaces.

On the sample treated for 300 minutes, the ferrite grains were elongated and connected, whereas the intermetallic phases were located preferentially on the grain boundaries. The grains thickness reached the minimum value, probably due to both the recrystallization phenomenon and the ferrite amount reduction, giving reason to a decrease in the ultrasound attenuation. The secondary phases are also present but the effect of these phases on the ultrasound velocity is probably less important than the grain refinement.

After 300 minutes of treatment, the thickness of the ferrite grains increased again, whereas the volume fraction of the ferrite phase continued to decrease. In addition, the volume fraction of the intermetallic phases went on to increase, not only on the grain boundary, but also within the grains. Otherwise, the secondary phases amount located into the grain were significantly less than that detected on the grain boundaries. For these reasons the attenuation could be explained by two different concomitant phenomena: the first is the ferrite grain growth and the second is the reduction of ferrite amount due to the secondary

phases growth. Thus, despite the complex transformation experienced by the investigated material, it seems that during the ferrite transformation two mechanisms contribute to rule the UTs attenuation. The first mechanism may be related to the formation of new grain boundaries in the ferrite phase at short treatment times. The second mechanism is the formation of new rounded grains of austenite and the reduction of ferrite phase at high treatment times [27].

The misorientation analysis shows a progressive decrease of the misorientation angles in all the studied conditions, except at 300 minutes, where the measurement about CSL shows that $\Sigma 13/\Sigma 3$ ratio is larger than for others conditions, indicating that in this condition the recrystallization takes place again, confirming the previous hypothesis.

The material featured by finer grains is interested by a lower attenuation of ultrasound (the ultrasound velocity increased in this condition) [26]. Thus, for 300 minutes of treatment time, the attenuation is lower than other conditions, even though in presence of intermetallic phases, because the microstructure consists of finer grains and consequently, the ultrasound velocity is larger.

The performed tensile tests pointed out the mechanical behavior of the material containing the intermetallic phases. The obtained results about the elastic modulus showed small variation between the different conditions, even if at 300 minutes of treatment time, the value of this mechanical feature increases and this behavior is consistent with the presence of intermetallic phases and the grains of microstructure more finer than grains in others conditions. This trend is similar to that revealed for the ultrasound velocity suggesting a relationship between this parameter and elastic modulus. However, a reliable explanation about the effect of precipitation on elastic properties of UNS S31803 duplex stainless steel still lacks and further investigations are needed to completely understand the relation among precipitation, phase morphology, Young modulus and longitudinal ultrasound velocity. For these reasons the ultrasound velocity behavior could be explained now as a result of many effect, at microscopic scale and in particular due to the grain size and the variation in Young modulus. However, these results show that despite other factors that complicate attenuation measurements i.e., surface roughness, sample geometry of real cases, it is possible to use UTs to characterize microstructural changes produced by isothermal heat treatments and can be a very useful non-destructive tool to monitor the transformation of ferrite phase and the precipitation of secondary phases (χ , σ , γ'') that affects the mechanical and corrosion properties of 2205 duplex stainless steel.

CONCLUSIONS

The response of a duplex stainless steel inspected by ultrasound technique changes as a function of the applied heat treatment time, according to the morphology and volume fraction of the phases featuring the microstructure.

For larger grains on the microstructure, the attenuation on the ultrasound beam is important and consequently, decrease the ultrasound velocity. On the other hand, for smaller grains, the attenuation decrease, increasing the ultrasound velocity of material.

Thus, the ultrasound velocity is significantly affected by the grain size of the ferrite phase, the volume fraction of the intermetallic phase precipitated within the duplex stainless steels and the elastic modulus of the material.

REFERENCES

- 1) J.-B. VOGT, *Mater. Proc. Tech.*, **117**, (2001), p.364.
- 2) A. MATEO, L. LLANES, N. AKDUT, M. ANGLADA, *Mater. Sci. Eng. A*, **319-321**, (2001), p.516.
- 3) J. CHARLES, *Weld. World (UK)*, **36**, (1995), p.43.
- 4) J. CHARLES, DUPLEX STAINLESS STEELS, A REVIEW AFTER DSS '07 HELD IN GRADO, proceeding of Duplex International Conference and Expo 2007, 18-20 June 2007, Grado, Italy.
- 5) H.S. CHO, L. KWANGMIN, *Mater Charact*, **75**, (2013), p.29.
- 6) J. MICHALSKA, M. SOZANŃSKA, *Mater Charact*, **56**, (2006), p.355.
- 7) K.H. LO, C.H. SHEK, J.K.L. LAI, *Mater. Sci. Eng. R*, **65**, (2009), p.39.
- 8) T.H. CHEN, J.R. YANG WENG, *Mater. Sci. Eng. A*, **338**, (2002), p.259.
- 9) A. S. TOPOLSKA, B. J. ŁABANOWSKI, *JAMME*, **96-2**, (2009).
- 10) S.K. GHOSH, S. MONDAL, *Mater Charact* **52**, (2008), p.1776.
- 11) N. LOPEZ, M. CID, M. PUIGGALI, *Corros Sci*, **41**, (1999), p.1615.
- 12) AA.VV., Le prove non distruttive. Associazione Italiana Metallurgia - Centro prove non distruttive, Milano (1999).
- 13) J. KRAUTKRAMER, *Ultrasonic Nondestructive Testing of Materials*. Defense Technical Information Center, (1952).
- 14) D. K. PANDEY, S. PANDEY, in *Ultrasonics: A Technique of Material Characterization, Acoustic Waves*, Don Dissanayake (2010), p.414.
- 15) U.F. KOCKS, C.N., H.R. TOMÉ WENK, *Textures and Anisotropy*. Cambridge University Press, Cambridge (1998), p.205.
- 16) AA.VV., *ASM Metals Handbook Volume 17, Nondestructive Evaluation and Quality Control*, Materials Park (Ohio), ASM International (1992), p.345.
- 17) D.M. ESCRIBA, E. MATERNA-MORRIS, R.L. PLAUT, A.F. PADILHA. *Mater Charact*, **60**, (2009), p.1214.
- 18) R. MAGNABOSCO, *Materials Research*, **12-3**, (2009), p. 321
- 19) M. POHL, O. STORZ, T. GLOGOWSKI, *Mater Charact*, **58**, (2007), p.65.
- 20) I. CALLIARI, M. ZANESCO, E. RAMOUS, *J Mater Sci* **41**, (2006), p.7643.
- 21) L.A. NORSTROM, S. PETERSON, S. NORDINI, *Z. Werkstofftech.*, **12**, (1981), p.229.
- 22) Y. MAEHARA, Y. OHMORI, J. MURAYAMA, N. FUJINO, T. KUNITAKE, *Met. Sci.*, **17**, (1983), p.541.
- 23) F.J. HUMPHREYS AND M. HATHERLY, *Recrystallization and Related Annealing Phenomena*, Elsevier (2004).
- 24) D.Y. KOBAYASHI, S. WOLYNIEC, *Mater. Res.*, **2-4**, (1999), p.239.
- 25) A.R. AKISANYA, U. OBI, N.C. RENTON, *Mater. Sci. Eng. A*, **535** (2012), p. 281-289
- 26) S. BARELLA, A. GRUTTADAURIA, C. MAPELLI, D. MOMBELLI, C.L. FANEZI, F. FIOLETTI, M. FORMENTELLI, M. GUARNERI, *Adv. Eng. Mater.*, **16-1**, (2013), p.103.
- 27) A. RUIZ, N. ORTIZ, H. CARREÓN, C. RUBIO, *J. Nondestruct. Eval.* **28**, (2009), p.131.

Studio sull'influenza della microstruttura nei test ultrasonori su componenti forgiati in acciaio duplex

Parole chiave: Acciaio inossidabile duplex - Forgiatura - Prove non distruttive - Ispezione ad ultrasuoni - Attenuazione - Fasi intermetalliche

I controlli ultrasonori sono fondamentali per garantire l'integrità dei manufatti metallici, specialmente per i grandi componenti ottenuti per forgiatura. A causa dell'elevata attenuazione che gli acciai inossidabili duplex generano sull'onda sonora, i controlli ad ultrasuoni condotti su questi tipi di acciai perdono spesso di efficacia, rendendo molto difficile l'ispezione. In questo lavoro è stata studiata l'interazione fra la radiazione acustica ultrasonora emessa da una sonda a 4 MHz e la microstruttura dell'acciaio inossidabile duplex grado 2205. Diversi campioni, ricavati da una barra forgiata e solubilizzata, sono stati trattati a 780 °C per tempi differenti al fine di promuovere la precipitazione delle fasi intermetalliche χ e σ . I forgiati in duplex di grandi dimensioni possono, infatti, soffrire di una residua frazione di fasi intermetalliche causata dai successivi cicli di riscaldamento necessari tra un passo di forgiatura e l'altro, e risulta pertanto importante capire come questi precipitati influenzino la risposta agli UT durante i controlli non distruttivi.

La risposta ultrasonora dei diversi campioni è stata misurata e correlata con le variazioni microstrutturali indotte dai trattamenti isotermi proposti. I campioni sono stati inoltre caratterizzati dal punto di vista cristallografico mediante tecnica EBSD per determinare le orientazioni e le tessiture cristallografiche e relazionarle con l'attenuazione dell'onda ultrasonora. I campioni sono stati inoltre caratterizzati dal punto di vista meccanico per determinare come la precipitazione delle fasi intermetalliche influenzi il comportamento del materiale.

I diversi tempi di mantenimento a 780 °C hanno permesso di determinare la dinamica di precipitazione e le modalità di nucleazione e accrescimento delle diverse fasi secondarie. Attraverso tecniche di analisi dell'immagine sono state determinate le frazioni delle diverse fasi caratterizzanti la microstruttura dell'acciaio al variare del tempo di trattamento. La variazione della velocità ultrasonora longitudinale al variare del tempo di trattamento risulta dipendente dalla frazione volumetrica delle fasi intermetalliche e dalla morfologia dei diversi costituenti strutturali che caratterizzano il materiale. Le trasformazioni metallurgiche che hanno interessato il materiale hanno permesso di spiegare il comportamento meccanico e ultrasonoro del materiale. La concomitante presenza di fenomeni metallurgici quali ricristallizzazione, precipitazione e diffusione influenzano fortemente l'attenuazione che il materiale oppone al passaggio dell'onda sonora. A 300 minuti di trattamento si è ottenuta una configurazione microstrutturale in grado di ridurre al minimo il livello di attenuazione, registrando il valore più elevato di velocità sonica longitudinale del materiale.